

We are IntechOpen, the world's leading publisher of Open Access books Built by scientists, for scientists

6,900

Open access books available

186,000

International authors and editors

200M

Downloads

Our authors are among the

154

Countries delivered to

TOP 1%

most cited scientists

12.2%

Contributors from top 500 universities



WEB OF SCIENCE™

Selection of our books indexed in the Book Citation Index
in Web of Science™ Core Collection (BKCI)

Interested in publishing with us?
Contact book.department@intechopen.com

Numbers displayed above are based on latest data collected.
For more information visit www.intechopen.com



Passively Stabilized Doubly-Resonant Brillouin Fiber Lasers

Vasily V. Spirin, Patrice Mégret and Andrei A. Fotiadi

Additional information is available at the end of the chapter

<http://dx.doi.org/10.5772/61714>

Abstract

We consider ultra narrow-line lasers based on doubly-resonant fiber cavities, describe experimental techniques, and present two methods for passive stabilization of single-frequency fiber Brillouin lasers. In the first approach, Brillouin fiber laser is passively stabilized at the pump resonance frequency by employing the self-injection locking phenomenon. We have demonstrated that this locking phenomenon delivers a significant narrowing of the pump laser linewidth and generates the Stokes wave with linewidth of about 0.5 kHz. In the second methodology, the fiber laser is stabilized with an adaptive dynamical grating self-organized in un-pumped Er-doped optical fiber. The laser radiates a single-frequency Stokes wave with a linewidth narrower than 100 Hz. The ring resonators of both presented lasers are simultaneously resonant for the pump and the Stokes radiations. For adjusting the double resonance at any preselected pump laser wavelength, we offer a procedure that provides a good accuracy of the final resonance peak location with ordinary measurement and cutting errors. The stable regime for both Brillouin lasers is observed during some intervals, which are interrupted by short-time jumping-intervals. The lasers' stability can be improved by utilizing polarization-maintaining (PM) fiber configuration and a cavity protection system.

Keywords: Brillouin fiber laser, self-injection locking, ring fiber resonator

1. Introduction

Stimulated Brillouin Scattering (SBS) is the nonlinear process with the lowest threshold in optical fibers [1]. SBS in optical fiber is very valuable for numerous applications such as fiber lasers, fiber amplifiers, fiber sensors, and optical processing of radio-frequency signals [2-9].

Recently developed Brillouin fiber lasers with the so-called doubly-resonant cavity (DRC) demonstrate low threshold, high spectral purity, and low intensity noise [10]. These lasers are

very promising for a variety of special uses, such as coherent interferometric sensing, optical communication, microwave photonics, and coherent radar detection [11-13].

The Stokes wave in these lasers is generated within a short fiber ring cavity, which is simultaneously resonant for the pump and the Stokes radiations. This configuration also delivers the minimal Brillouin threshold. However, stable operation of the DRC Brillouin laser is extremely sensitive to the resonance detuning between the pump frequency and the ring cavity mode. Typically, in order to obtain an established single-longitudinal mode (SLM) operation, various types of active stabilization systems that adjust the cavity length or alter the frequency of the pump laser are used [11-12].

In Sections 3 and 4, we report two schemes of passively stabilized SLM DRC Brillouin lasers.

1. In the first scheme, the single-mode doubly-resonant Brillouin fiber laser is passively stabilized at the pump resonance frequency by employing the self-injection locking phenomena. Optical self-injection locking has drawn a lot of attention for optical communication application as an efficient technique to improve the spectral and polarization properties of semiconductor lasers [14-16]. The physical phenomena observed with optical feedback in DFB varied from linewidth narrowing with weak feedback to irregular chaotic oscillations with the strong one [14,17]. In this work, we utilize self-injection locking for matching the DFB pump laser frequency with the Brillouin laser resonance cavity mode as well as for decreasing the pump laser linewidth.
2. In the second approach, the pump fiber laser is stabilized with a population inversion grating imprinted in an un-pumped Er-doped optical fiber.

In Section 2, we present a special procedure for the precise setting of the ring fiber cavity to the double resonance condition at any preselected pump wavelength. We show that experimental record of the cavity Brillouin response to a frequency scan of the pump laser allows calculating the excess ring cavity length that must be removed from the ring in order to shift the Brillouin resonance to the right position. We have demonstrated that the proposed algorithm delivers a good accuracy of the resonance peak location with ordinary measurement and cutting errors.

2. Adjustment of double resonance in Brillouin fiber lasers

Doubly-resonant Brillouin laser cavity should be simultaneously resonant for the pump and the Stokes radiations. The free spectral range (FSR) of the fiber cavity with a length of about several meters is equal to tenths of MHz. Therefore, typical pump DFB laser can be easily adjusted to a cavity mode by current or temperature setting. The problem then is how to keep this matching despite random deviations of the cavity length and/or pump laser frequency. However, even if we provide precise and stable coincidence of the pump laser frequency with one of the cavity resonant modes, it does not guarantee the resonance for the down-shifted Stokes wave for short cavities.

In this paragraph, we present an algorithm and an experimental technique for the adjustment of the double resonance of the fiber optical ring cavities at any preselected wavelength. The experimental setup is depicted in Fig. 1.

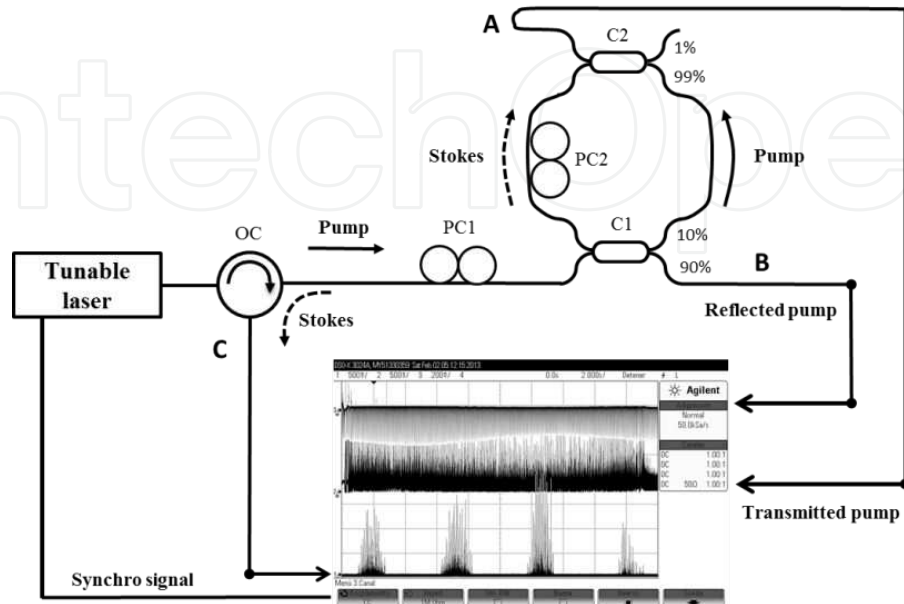


Figure 1. Double resonance peaks recorded with single wavelength scan.

A fiber ring cavity with the lengths about 4 m is pumped by a tunable laser Agilent 81940A with 100 kHz linewidth and output power up to 25 mW. The behavior of the fiber-optic ring resonator is very similar to a linear Fabry-Perot cavity, so the ports B and A are equivalent to the reflected and the transmitted ports of the linear cavity, respectively. Figure 1 also illustrates how the double resonance looks in the experiment. When the tunable laser sweeps in the interval 1540–1560 nm synchronously with oscilloscope trace, the Stokes peaks appear only for the certain pump wavelengths that correspond to the double resonance condition.

The length L of the fiber inside the ring defines the FSR of the cavity:

$$FSR = c / nL, \quad (1)$$

where c is the speed of light in a vacuum, and n is the refractive index of the SMF-28 fiber equal to 1.468 at 1550 nm [18].

The double resonance is achieved when the Brillouin shift ν_B is equal to an integer multiple of the FSR (see Fig. 2):

$$\nu_B = m FSR, \quad (2)$$

where m is an integer, which here we refer to as the order of the Stokes peak.

With this condition, the cavity became resonant for both the pump and Stokes radiations, which drastically reduces the SBS threshold and leads to Stokes peaks emergence.

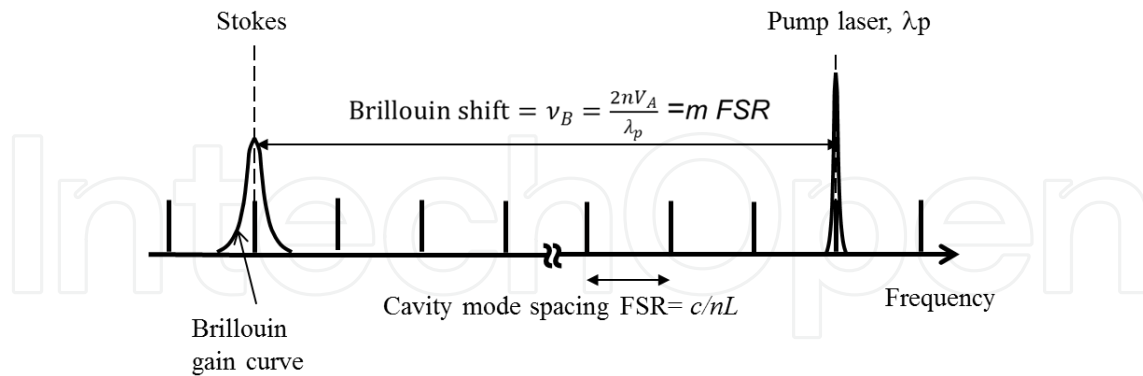


Figure 2. Doubly-resonant conditions.

In order to find the doubly-resonant states, we adjust the Brillouin shift by tuning the wavelength of the pump laser λ_p , because the Brillouin shift depends on pump wavelength as:

$$\nu_B(\lambda_p) = \frac{2nV_A}{\lambda_p}, \quad (3)$$

where $V_A \approx 5800$ m/s [19] is the acoustic velocity in the optical fiber.

For a precise measurement of the acoustic velocity, we have developed the experimental setup presented in Fig. 3. The radiation of the tunable laser at a fixed wavelength equal to 1549.7 nm was injected into the cavity ring through the circulator OC and the coupler C1. This wavelength was chosen to lead to Stokes emission in the ring cavity. The beat frequency between the Stokes component and the backscattered Rayleigh radiation of the pump is registered at port A with an RF spectrum analyzer HP 70908A. This beat frequency was found to be equal to 10.87689 GHz, which gives us with eq. 3 an acoustic velocity equal to 5740 m/s, so very close to the expected theoretical value.

The resonant coupling between the scanning pump laser and the cavity mode occurs during very short multiple time intervals. Indeed, the increase of the transmitted pump power at the resonance is accompanied by a decrease of the reflected power as shown in Fig. 4. Strong pulses at the Stokes wavelength are recorded at port C when the pump power is sufficient to exceed the Brillouin threshold. These pulses are red-shifted by ~ 0.08 nm from the pump wavelength and can only appear when the Brillouin frequency shift is an integer multiple of the FSR. Moreover, there is a perfect synchronization between these Stokes pulses and the transmitted ones. This is precisely the double resonance condition.

In order to estimate the exact position of the double resonance peaks, we use an averaging procedure. Envelopes of the Stokes pulses after averaging of 7 laser scans, recorded for initial unadjusted cavity, are shown in Fig. 5.

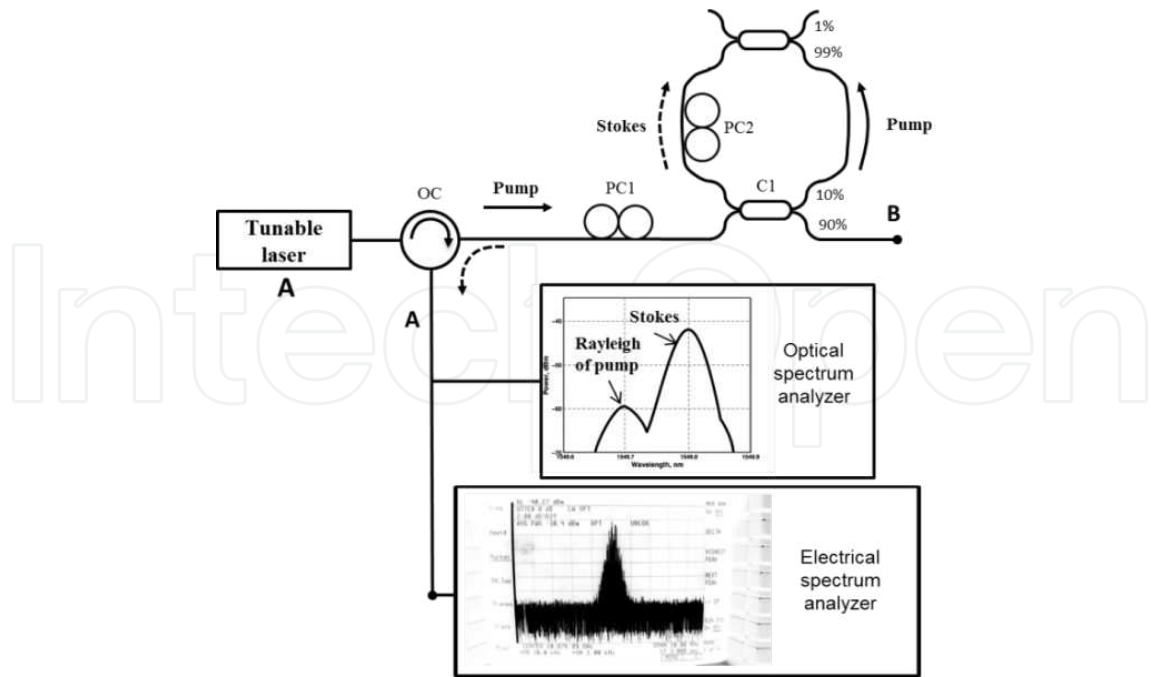


Figure 3. Experimental setup for precise acoustic velocity measurement.

The order of the envelope peak m can be found from the eqns. (1–3) as the nearest integer function [20]:

$$m = \text{rint} \left(\frac{\lambda_{m-1}}{\lambda_{m-1} - \lambda_m} \right), \quad (4)$$

where λ_m, λ_{m-1} are the central wavelengths of the neighboring m and $(m-1)$ – orders of the envelopes inside the measuring interval.

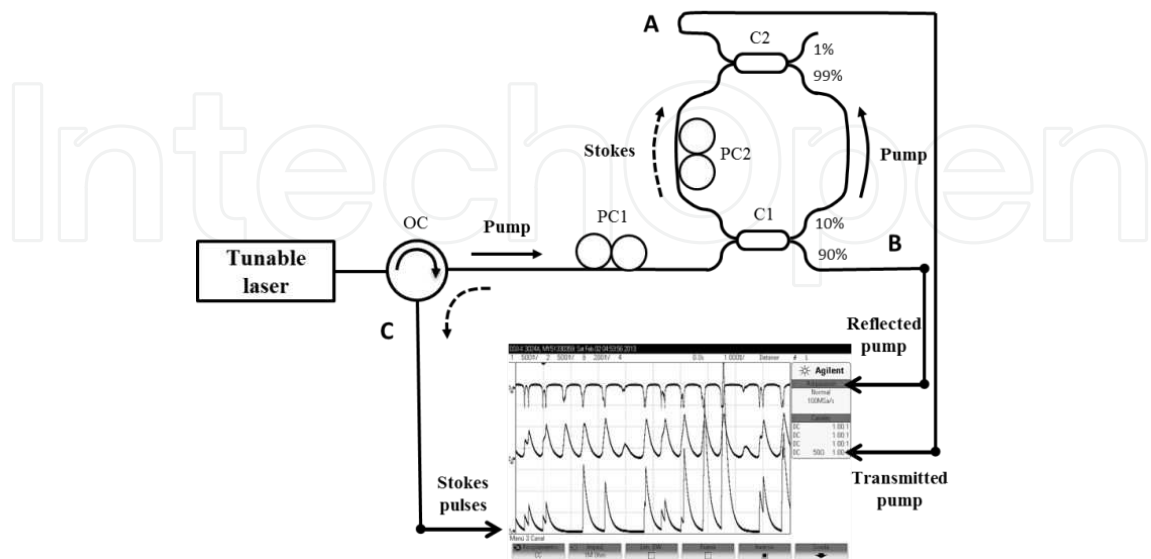


Figure 4. Signals at double resonance during the scanning.

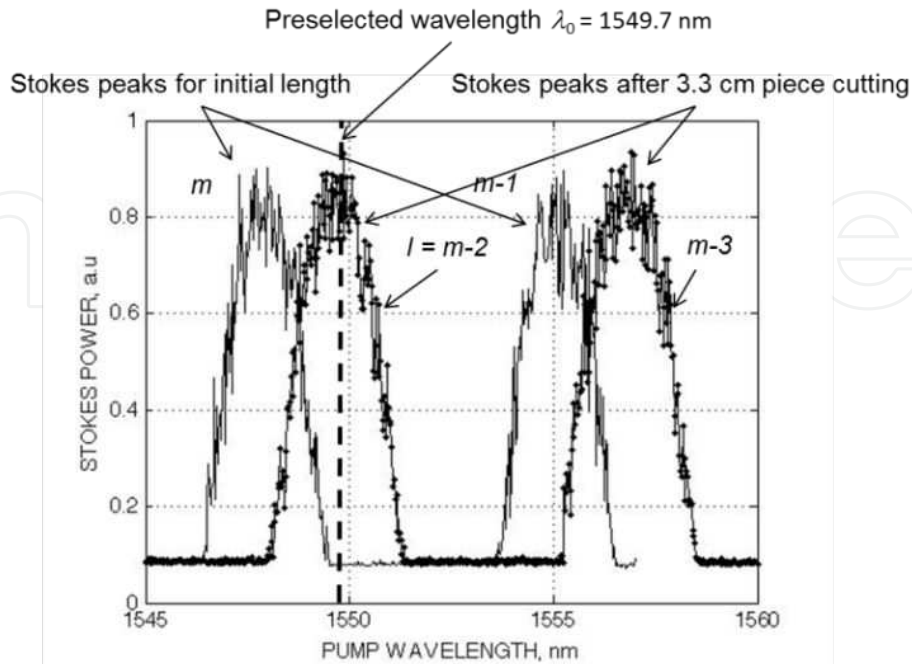


Figure 5. Stokes envelopes vs. pump wavelength after 7 scans averaging for initial and adjusted cavities.

The DFB pump laser we use in the Brillouin ring laser has a fixed wavelength equal to 1549.7 nm. As we see from Fig. 5, the envelope positions for unadjusted cavity are noticeably away from the wanted wavelength $\lambda_0 = 1549.7$ nm. The nearby peaks to λ_0 Stokes envelopes have central wavelengths equal to 1547.9 nm and 1555 nm, which corresponds to $m = 219$ and $m-1 = 218$, respectively (see Fig. 5).

From the eqns. (1–3), we find that to move the l -order envelope peak, calculated for the original cavity, to its new position with the central wavelength equal to λ_0 , we should reduce the cavity length by ΔL :

$$\Delta L = \frac{c}{2n^2V_A} (m\lambda_m - l\lambda_0), \tag{5}$$

Figure 6 shows the lengths ΔL calculated for our experimental data as a function of $m-l$. In theory, we can move to the new position any envelope peak that is located at the right side from λ_0 [20]. For example, we can move at the required position the nearest 218-order peak ($m - l = 1$), but technically it is difficult to splice the fiber when cutting less than 2-cm piece of the fiber. In the experiment, we replace the 217-order peak ($m - l = 2$) to the preselected wavelength 1549.7 nm, by cutting $\Delta L = 3.3$ cm piece of the fiber. As we can see in Fig. 5, the result of the adjustment is in good agreement with the analytical estimation.

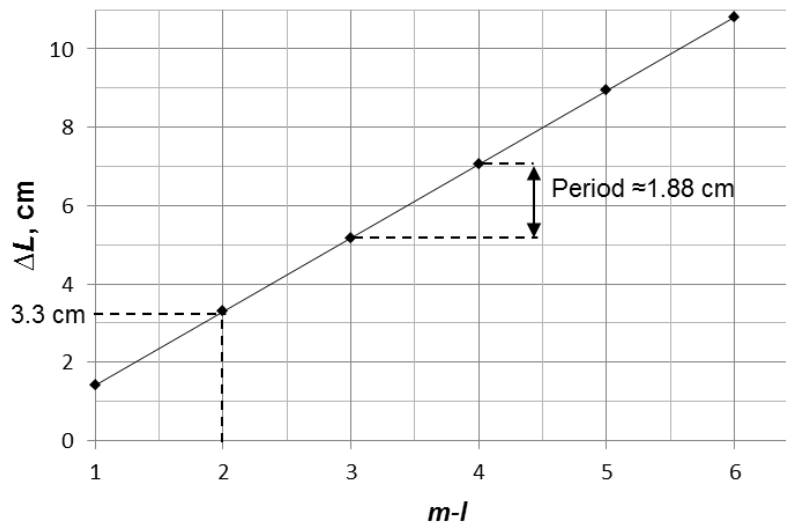


Figure 6. Cutting length ΔL vs. difference in peak orders $m-l$.

Let us now consider the uncertainties of the algorithm for adjusting the doubly-resonant condition in the ring Brillouin fiber laser. The cavity adjustment algorithm includes three main steps:

1. Experimental recording of the Brillouin traces with the original cavity. Determination of the Stokes envelope positions.
2. Calculation of the length ΔL , which must be taken out from the cavity in order to transfer the resonance peak to the preselected position.
3. Cutting and splicing the fiber into the cavity in order to reduce the cavity length by ΔL .

Each of these actions introduces some errors that decrease the accuracy of the technique [21].

The experimental determination of the central wavelengths of the envelopes λ_{m-1} , λ_m is accompanied by some errors $\delta\lambda_{m-1}$, $\delta\lambda_m$ which depend on the accuracy of the equipment used to measure the wavelength. The standard uncertainty of the peak order m can be estimated from eqn. (4) with the error propagation formula as:

$$\delta m = \frac{\sqrt{2}\lambda_m}{(\lambda_{m-1} - \lambda_m)^2} \delta\lambda_m, \quad (6)$$

where $\delta\lambda_{m-1} = \delta\lambda_m = \delta\lambda$ are the standard errors in determination of the peak location.

The ordinary error of the peak position $\delta\lambda$ in our experiment is equal to 0.1 nm; however, with additional averaging over a number of oscilloscope traces, we get an uncertainty equal to 0.05 nm. Even higher precision can be obtained because the tunable laser Agilent 81940A is arranged for typical absolute wavelength accuracy equal to ± 5 pm with repeatability ± 1 pm.

Figure 7 shows the standard error of m versus the cavity length L for different accuracies of the peak position measurement. The dependence is calculated utilizing eqns. (6) and (1–3) for λ_m equal to 1550 nm. The method delivers absolutely correct value of the peak order only for the very short cavities. For the cavities with lengths 4.0–8.0 m, the uncertainty of m reaches 1–2%. Nevertheless, the relatively high error of the peak order m makes minor contribution to the final error of the adjusted resonance peak position.

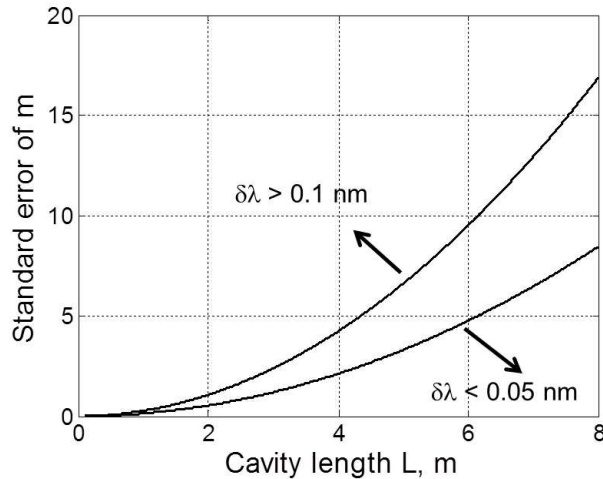


Figure 7. Standard error in calculations of Stokes peak order m .

Without loss of generality, we can assume that we transfer the $(m-1)$ order peak toward the preselected position, which is located between the m and $(m+1)$ order peaks. With this assumption, the maximum standard uncertainty of the required length reduction ΔL can be estimated as:

$$\delta\Delta L \cong \frac{c}{2n^2V_A} \left(\frac{\sqrt{5}\lambda_m}{\lambda_{m-1} - \lambda_m} \right) \delta\lambda \quad (7)$$

Figure 8 shows the uncertainty $\delta\Delta L$ versus the length of the laser cavity L . The errors in the estimation of the cutting piece ΔL are less than 0.6 mm for the 0.1 nm error in the position of the resonance peak for 4 m-length fiber cavity.

Now with eqn. (5) we can estimate the inaccuracy in the position of the $(m-1)$ order peak which we move at desired wavelength λ_0 . The resulting errors in the position of the peak due to cutting and measurement errors are shown in Fig.9.

The error in the position of the adjusted peak due to measurement errors is equal to 1.6 MHz. This error is thus significantly less than the linewidth of Brillouin gain profile in the fiber, which is equal to about 30 MHz. However, the main errors of the method occur due to inaccuracies of the cut-splice procedure. Fortunately, even for the 1 m-long fiber cavity with

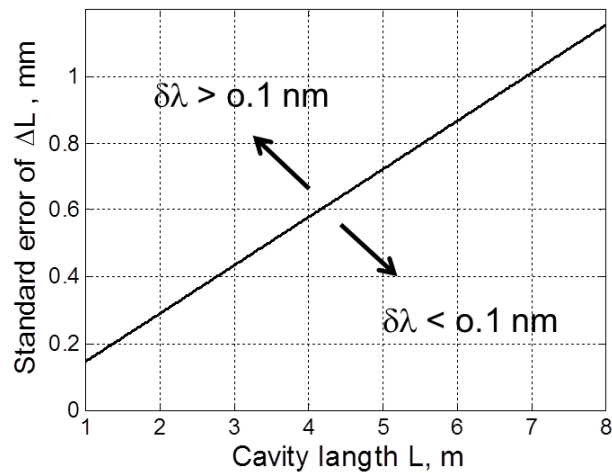


Figure 8. Standard error in estimations of cavity reduction length ΔL .

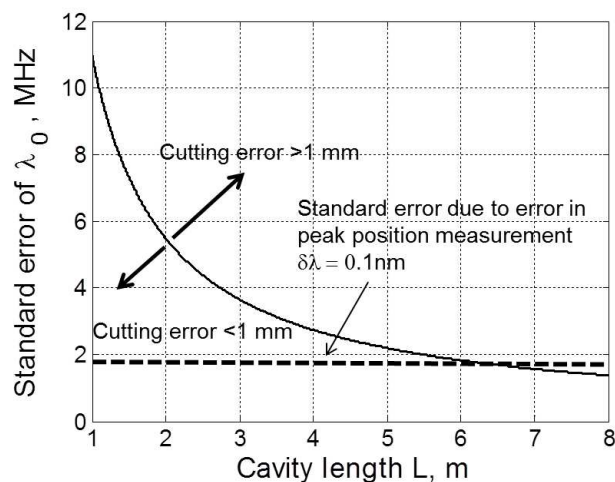


Figure 9. Standard error of the adjusted peak position.

1 mm cutting error, we get only an error of 11 MHz in the final peak position, which is quite reasonable for practical applications. Therefore, the algorithm provides good precision for the adjusted peak location with ordinary measurement and cutting accuracy.

Besides the adjustment of the double resonance, the proposed technique allow finding of the fiber cavity length:

$$L = \frac{c}{2n^2V_A} \left(\frac{\lambda_m \lambda_{m-1}}{\lambda_{m-1} - \lambda_m} \right). \quad (8)$$

However, the error in the length estimation with eqn. (8) is relatively high. Figure 10 shows the standard errors in the estimation of the fiber cavity length, which was calculated utilizing

eqn. (8) with error propagation formula. The standard uncertainty of the cavity length exceeds 30 cm for the 8-m-length cavity and 0.1-nm errors in the peak position measurement. Thus, more precise measurement of the peak location is required for the accurate determination of the cavity length with this method.

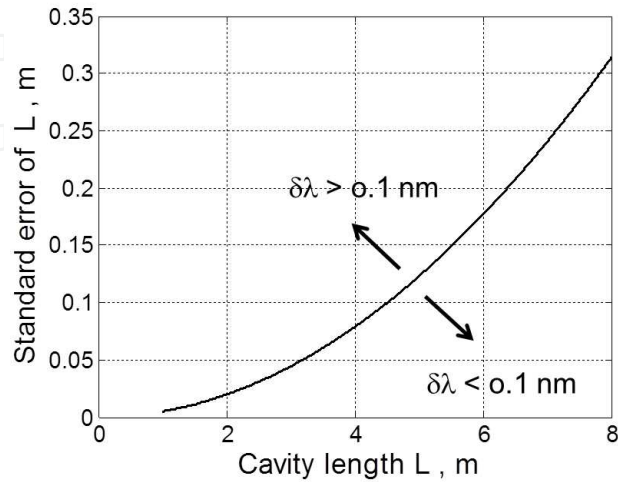


Figure 10. Error of the estimation of the cavity length.

3. Doubly-resonant Brillouin fiber laser passively stabilized with self-injection locking phenomena

In this section, we present a single-longitudinal-mode, doubly-resonant Brillouin fiber laser, which is passively stabilized at the pump resonance frequency by employing the self-injection locking phenomena.

The experimental configuration of this passively stabilized SLM Brillouin fiber laser is shown in Fig. 11. The Brillouin laser is pumped by a standard MITSUBISHI FU-68PDF-V520M27B DFB laser with a fiber output and a built-in optical isolator. The output radiation of pump laser, which operates at a wavelength equal to 1549.7 nm, is connected to the optical circulator OC1, amplified by an Er-doped fiber amplifier (EDFA) up to 30 mW and launched into the fiber-optic ring resonator (FORR) through another optical circulator OC2. The FORR comprises two couplers, polarization controller, and contains approximately 4-m-long fiber. The feedback switch (FS) provides the possibility to switch-on or switch-off the optical feedback signal reaching the DBF laser. The FORR was preliminary adjusted for double resonance at pump wavelength equal to 1549.7 nm by utilizing the algorithm described in the previous section.

Once the pump laser gets a resonance with the ring laser cavity, the growing optical feedback forces the DFB pump laser to operate at the cavity resonance frequency. After such locking, any slow detuning of the cavity resonance caused, for example, by temperature variations, is compensated by a matching deviation of the pump laser operation wavelength.

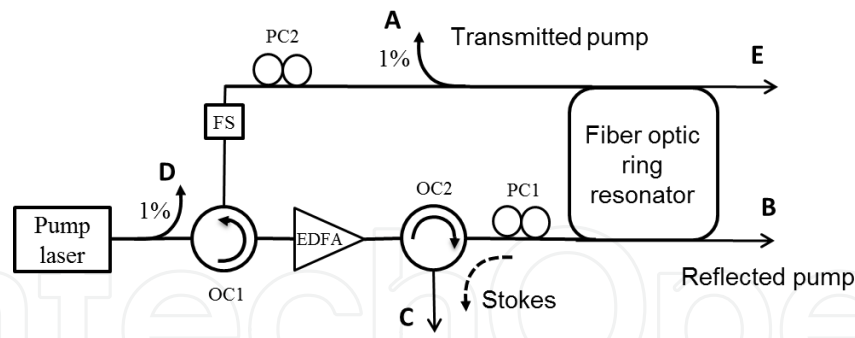


Figure 11. Configuration of the Brillouin laser with self-locked DFB pump laser; OC – optical circulator, PC – polarization controller, FS – feedback switcher.

The linewidth of pump laser was measured with the delayed self-heterodyne technique. An all-fiber spliced Mach-Zehnder interferometer with a 15-km delay fiber in one arm and 20 MHz phase modulator supplied by polarization controller in the second arm is used for this purpose. Figure 12 shows delayed self-heterodyne spectra of unlocked (Fig. 12a) and locked DFB (Fig. 12b) pump laser at port D of Fig. 11.

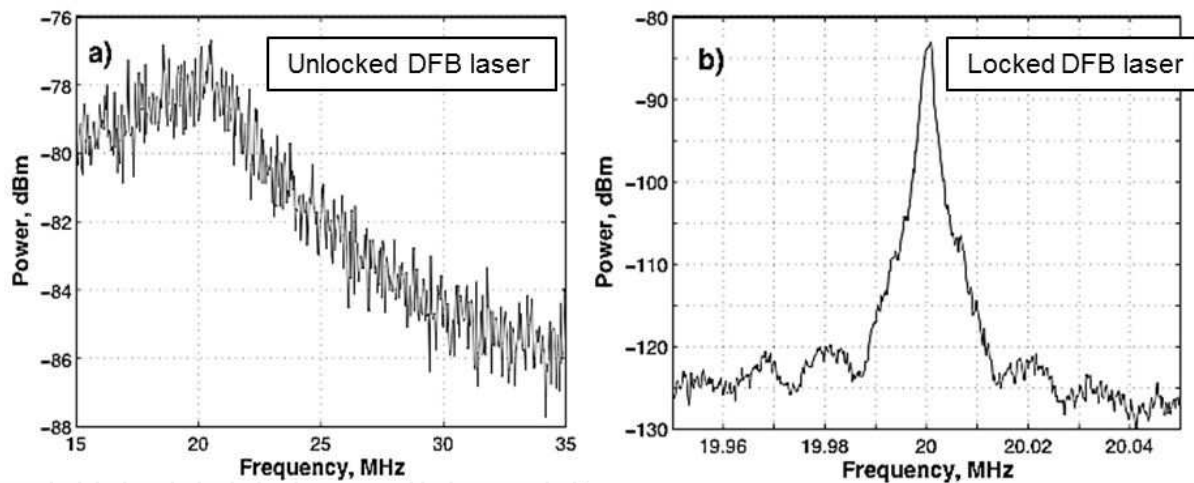


Figure 12. Delayed self-heterodyne spectra of the DFB pump lasers; a) unlocked laser, b) self-locked pump laser.

For the unlocked DFB laser, the full-width at half-maximum (FWHM) linewidth was estimated equal to 4 MHz, assuming that the line shape is Lorentzian. Meantime, the linewidth of the locked pump laser reduces by more than 1000 times (see Fig. 12b) [22].

With the resonance, the power, which is circulating inside the FORR, is increasing up to the Brillouin threshold. After the SBS threshold is reached, some of the pump energy is converted into a Stokes wave, traveling in the opposite direction inside the ring. The main part of the backward-propagating Stokes radiation is relaunched into the FORR but the other part goes out and is available at ports C and E.

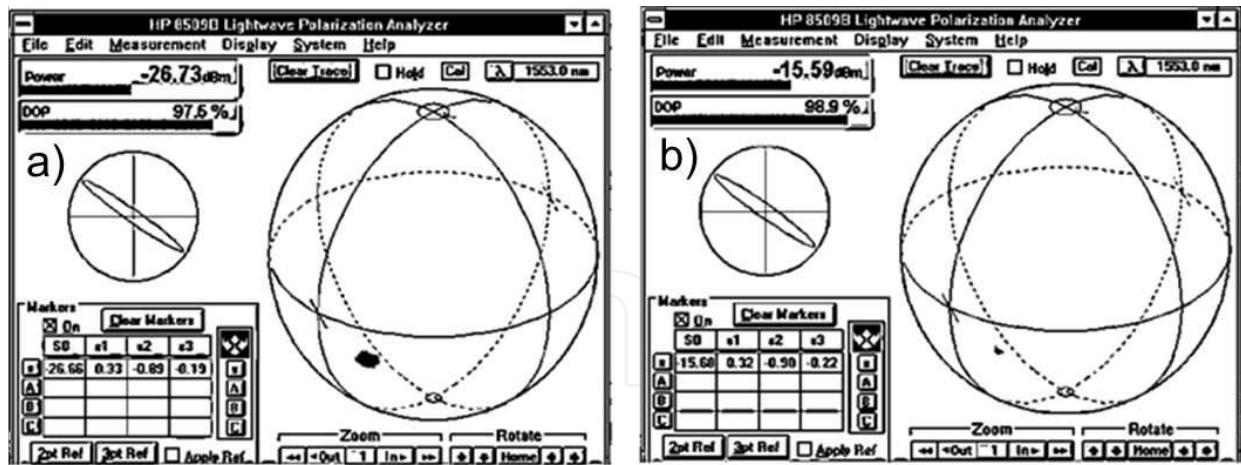


Figure 13. Polarization state during 30 s: a) unlocked, and b) locked DFB pump laser.

Figure 13 shows time-behavior of the polarization states of the unlocked and locked DFB pump laser recorded at port D during 30 s. The free running and locked laser emitted nearly completely polarized light with degree of polarization (DOP) equal to 98–99%. However, the locked laser demonstrates a slightly better temporal stability of the polarization. Whatever the feedback, the Stokes wave polarization significantly varies in time (see Fig. 14).

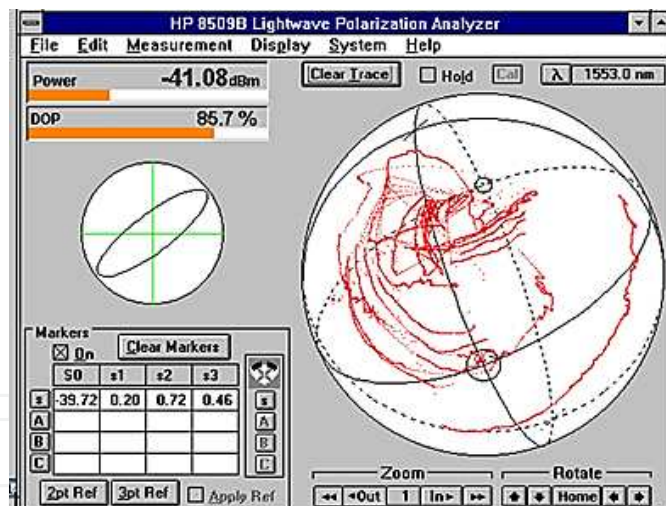


Figure 14. Polarization state of the Stokes radiation during 30 s.

The maximum output Stokes power at port C was about 5 mW providing approximately 40% Brillouin laser slope efficiency. The Stokes linewidth is expected to be narrower than the pump one [23]. Indeed, Fig. 15 shows the delayed self-heterodyne spectra of the Stokes component of the Brillouin laser from which the double linewidth $2\Delta\nu$ can be estimated to be equal to 10 kHz with 20 dB criterion that corresponds to 1 kHz with 3 dB criterion [24]. It should be noted that the delay length of 15 km is too short to obtain the incoherent mixing, which is required in the measurements utilizing delayed self-heterodyne technique. For the 0.5 kHz linewidth,

the length of the delay fiber should exceed 100 km. However, the error due to the shorter delay fiber can lead to visible large-scale oscillations in self-heterodyne spectra and an increasing of the estimated linewidth in comparison with actual one [24]. For this reason, the actual linewidth of the Brillouin laser is better than the measured value equal to 500 Hz.

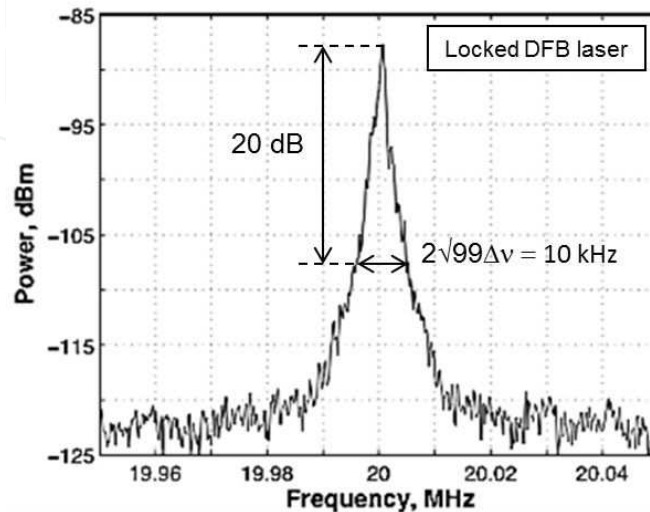


Figure 15. Delayed self-heterodyne spectra of the Stokes radiation of Brillouin laser.

Figure 16 illustrates a typical time-behavior of the Brillouin laser without locking. When optical-feedback (FS) is switched off, the injection locking of the pump laser is disabled and the stable resonance is never observed. Indeed, the pump power is almost totally reflected from FORR to port B. Without locking, the pump power inside the Brillouin laser cavity is small. So the transmitted pump power and the Stokes component are almost negligible at ports A and C, correspondingly.

On the other hand, optical feedback drastically changes the operation mode of the Brillouin laser (see Fig. 17). When FS is switched on, the Brillouin laser starts to operate mostly at the resonance mode of the FORR. The pump power mainly goes inside the FORR and the reflected power at port B becomes negligible. Analysis of the powerful single-frequency Stokes emission measured at port C shows that the observed regime consists of stable Stokes radiation for some duration, interrupted by short-time jumping intervals that are believed to be related to the hopping of the resonance mode of the fiber laser. It is clear that a more detailed analysis of this phenomenon is needed.

The variation of the transmitted pump power varies in antiphase with the reflected power, leading to a strong time correlation between the pump power and the Stokes radiation. The experimental conditions greatly modify the durations of the stable resonance-intervals and jumping-intervals. In the experiment presented here, ordinary SMF-28 fiber was used inside the FORR and the cavity was not stabilized against vibration and temperature. Under these conditions, stable Stokes radiation is usually observed during 0.5–5 s.

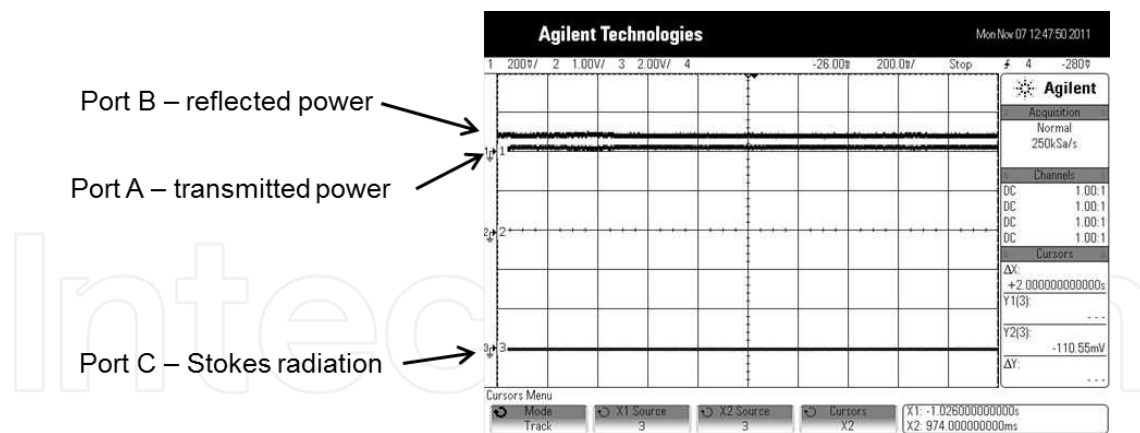


Figure 16. Oscilloscope traces when optical feedback is “switch-off.”

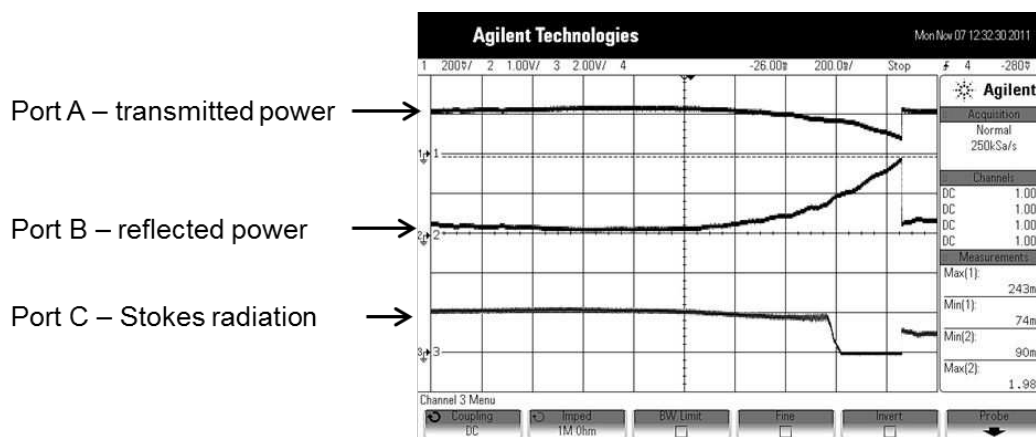


Figure 17. Typical oscilloscope traces when optical feedback is “switch-on.”

We believe that stability and efficiency of proposed technique can be noticeably improved with temperature stabilization and, for example, by utilizing polarization-maintaining fiber in the Brillouin ring cavity.

4. Brillouin fiber lasers passively stabilized with adaptive grating

In this section, we present another approach for passive stabilization of SLM DRC Brillouin laser that demonstrates even narrower laser linewidth than the one that was reported in the previous section. In this method, we utilize a population inversion grating, a side effect of the population inversion mechanism, which, along with the refractive index change effect, is widely used in many devices based on rare-earth doped fibers [25–32]. Here, dynamical grating is self-organized in the piece of the un-pumped Er-doped optical fiber and able to adjust the laser mode to the cavity resonance frequency. The adaptive all-fiber method was applied in combination with two coupled FORRs that were used for preliminary pump-mode selection and Stokes generation.

The experimental laser configuration is shown in Fig.18. Optical gain is supplied by a 4.5-m segment of erbium-doped single mode fiber (SM-EDF) pumped by 1480-nm laser diode through a 1480/1550 wavelength-division multiplexer (WDM). Optical circulator (OC) and two isolators (OI) provide unidirectional pump propagation through the cavity. To get single-frequency generation, the laser cavity also comprises two coupled FORRs.

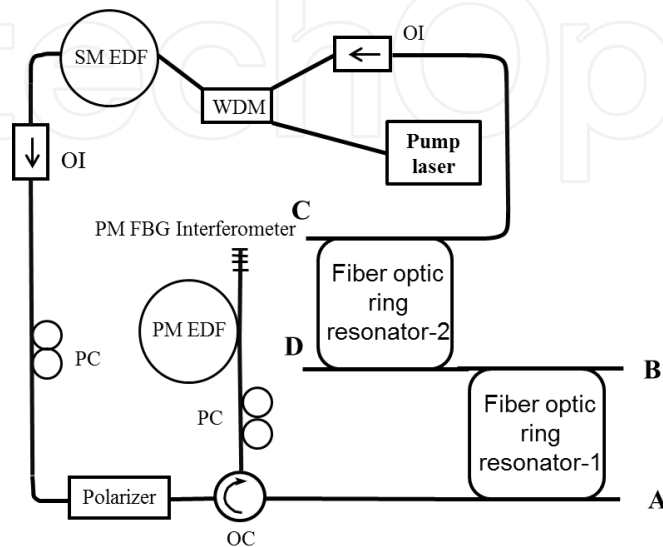


Figure 18. The laser configuration; OC- optical circulator, PC – polarization controller, OI – optical isolator, WDM – wavelength-division multiplexer, PM EDF – polarization-maintaining erbium-doped fiber, SM EDF – single-mode erbium-doped fiber.

This combined cavity has superior intermodal spacing, allowing the laser to operate only at modes that are common for both ring resonators, i.e., to suppress multilongitudinal-mode generation [33, 34]. The FORR-2 with a short fiber length is used only as a frequency-selective element only. High-fidelity FORR-1, comprising relatively long fiber, is used as a frequency-selective element and as the Brillouin laser ring cavity. The FORR-1 consists of two 95/5 couplers, polarization controller and contains 20-m length of a standard SMF-28 fiber used as an efficient media for Brillouin Stokes generation. The radiation at the Stokes wavelength is mainly emitted through port B, while port D is used to measure the parameters of the pump radiation. We install a fiber polarizer inside the main laser cavity that ensures single polarization mode of the pump radiation. A 1.7-m section of un-pumped erbium-doped polarization maintaining fiber (PM-EDF) has absorption of about 5.5 dB/m at 1530 nm and, in combination with the narrow-band fiber Bragg grating (FBG) interferometer, operates as an adaptive ultra-narrow-band reflector. The FBG interferometer is a Fabry-Perot cavity made of two uniform FBGs inscribed in the PM single mode optical fiber and separated by ~0.8 cm. It has 95% main reflectivity peak at 1547.37 nm with a FWHM equal to about 0.07 nm. In the course of this laser operation, the optical waves traveling in the un-pumped fiber section in opposite directions interfere to form a standing wave that causes inscription of a population inversion grating in the fiber. Indeed, the two-wave mixing effect [35] is the key phenomena used here to make the grating highly reflective at the inscribing light wavelength. The two-wave mixing being

strongly power-dependent, the grating reflectivity peak is enhanced at the laser resonance frequency and this high reflection reduces the cavity losses, leading to a further enhancement of the resonance frequency. Any slow detuning of the frequency, for example, due to temperature variation, is followed by the matching shift of the adaptive grating reflectivity peak.

The measured Brillouin threshold for this laser was about 4 mW. Optical spectra of the Brillouin laser recorded at the ports A and B with 5 mW pump power are shown in Fig. 19.

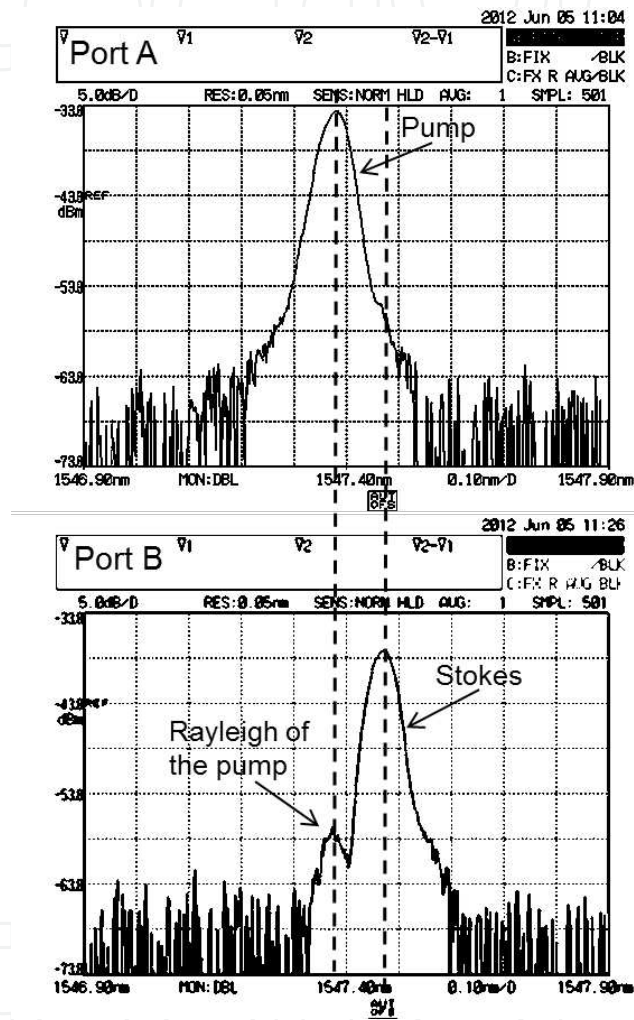


Figure 19. Brillouin laser optical spectra at ports A and B.

The Stokes power at port B was about 0.3 mW, providing approximately 30% slope efficiency of the pump-to-Stokes power conversion. The peak at the Stokes wavelength is about 20 dB higher than the peak associated with the Rayleigh scattering of the pump wave (see Fig. 19). Because of this high spectral contrast, this signal could be further amplified by an extra Er-doped amplifier without significant degradation of the signal-to-noise ratio.

The linewidths of pump and Stokes radiations were measured with the delayed self-heterodyne technique with a 25.3-km delay fiber in one arm and 15 MHz phase modulator in the

second arm. In this experiment, the beat signal is detected by a photodiode and an RF spectrum analyzer with a frequency resolution of about 100 Hz. Figure 20 shows the delayed self-heterodyne spectrum of the pump radiation recorded at port D. The pump FWHM is estimated to be 300 Hz. When increasing the pump power, the Stokes radiation appears at port B. As the pump frequency is resonant for FORR -1, the power circulating inside FORR -1 is about 35 higher than the power at the resonator input. This supports effective generation of the Brillouin radiation in FORR -1 comprising longer piece of fiber rather than FORR -2. The pump-to-Stokes power conversion efficiency is higher when FORR -1 is resonant not only for the pump, but also for the Stokes wave frequency. So, theoretically, we need to adjust the double resonance at FORR-1. However for the 20-m long cavity, the FSR is significantly smaller than the Brillouin gain width, so the resonance peaks are overlapping and this provides the double resonance without any adjustment [20].

The Stokes wave linewidth is expected to be narrower than the pump one. Figure 20 shows the delayed self-heterodyne spectrum of the Stokes wave that corresponds to a linewidth at half-maximum equal to about 100 Hz.

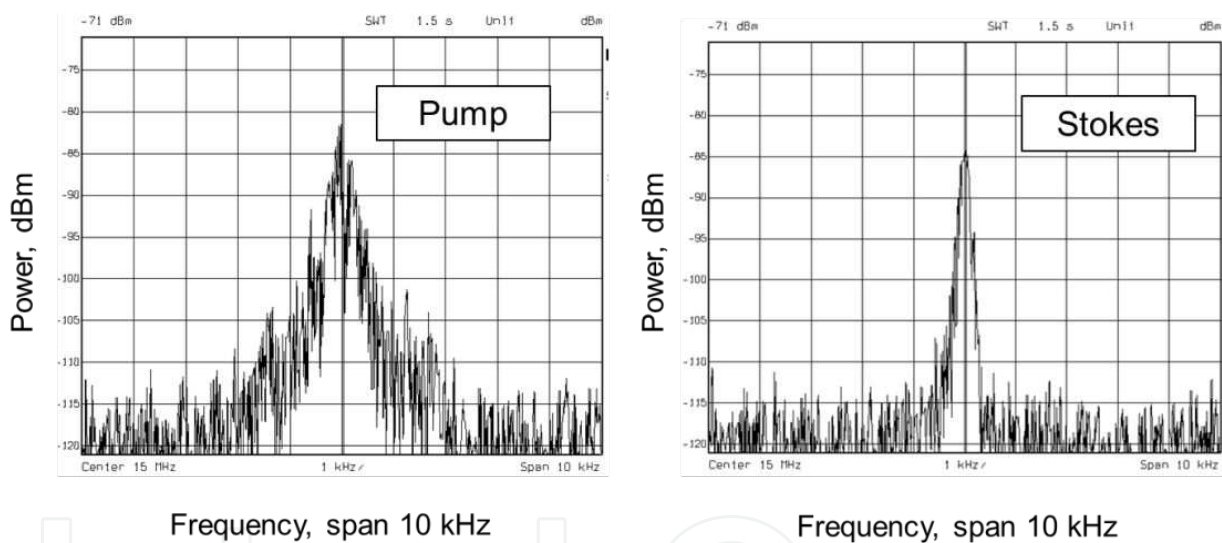


Figure 20. Delayed self-heterodyne spectra of the pump and Stokes radiations.

Typical time-behavior of this Brillouin laser is very similar to that reported before. Stable pump and Stokes power activities are observed during some time intervals that are interrupted by short-time jumping. There is a strong correlation between the time-behavior of the pump and Stokes radiations inside the cavities, where jumps of the pump power are always followed by Stokes power fluctuations. Moreover, below the Brillouin threshold, the Stokes radiation is negligible, but the laser dynamics is nearly the same as the one observed above the threshold. Environmental conditions strongly affect the stable interval durations and these stable durations could be significantly increased by an effective acoustic noise protection of the laser cavity. The stable time intervals of 0.2–1 s are typical for unprotected laser, which operates in regular lab environment [36].

5. Conclusion

We have presented two approaches for designing passively stabilized single-longitudinal-mode doubly-resonant Brillouin fiber lasers.

In the first approach, the SLM DRC Brillouin fiber laser is passively stabilized at pump resonance frequency by employing the self-injection locking phenomenon. For precise setting of the ring fiber cavity to the double resonance at any preselected pump laser wavelength, we design a special algorithm that delivers good accuracy of the resonance peak location with ordinary measurement and cutting errors. We have demonstrated that the locking phenomenon decreases the pump laser linewidth by a factor more than 1000 times and generates a Stokes wave with linewidth of about 0.5 kHz.

In the second approach, the pump fiber laser is stabilized with adaptive grating recorded in un-pumped Er-doped optical fiber. The laser is shown to emit a single-frequency Stokes wave with a linewidth narrower than 100 Hz. This result is a significant progress in the field of passively stabilized Brillouin lasers.

The stable regime for both Brillouin lasers is observed during some intervals that are interrupted by short-time jumping-intervals. We believe that the laser stability can be further improved by utilizing fully polarization-maintaining fiber spliced configuration and a proper cavity protection system.

Acknowledgements

We gratefully acknowledge financial support from the CONACYT, Mexico; the IAP program VII/35 of the Belgian Science Policy; and the Ministry of Education and Science of the Russian Federation (14.Z50.31.0015).

Author details

Vasily V. Spirin^{1*}, Patrice Mégret² and Andrei A. Fotiadi^{2,3,4}

*Address all correspondence to: vaspir@cicese.mx

1 División de Física Aplicada, CICESE, Ensenada, B.C., México

2 University of Mons, Electromagnetism and Telecommunication Department, Mons, Belgium

3 Ioffe Physico-Technical Institute of the RAS, St. Petersburg, Russia

4 Ulyanovsk State University, Ulyanovsk, Russia

References

- [1] Agrawal G.P.: *Nonlinear Fiber Optics*. 3rd ed., Academic Press, San Diego, 2001, 1-466.
- [2] Cowle G.J., Stepanov D. Yu.: Hybrid Brillouin/erbium fiber laser. *Opt. Lett.* 1996; 21: 1250-1252.
- [3] Fotiadi A.A., Mégret P.: Self-Q-switched Er-Brillouin fiber source with extra cavity generation of a Raman supercontinuum in a dispersion shifted fiber. *Opt. Lett.* 2006; 31:1621-1623.
- [4] Boucon A., Fotiadi A.A., Mégret P., Maillotte H., Sylvestre T.: Low-threshold all-fiber 1000 nm supercontinuum source based on highly non-linear fiber. *Opt. Comm.* 2008; 281: 4095-4098.
- [5] Preda C.E., Fotiadi A.A., and Mégret P.: Numerical approximation for Brillouin fiber ring resonator. *Opt. Express.* 2012; 20, 5783-5788.
- [6] Gruk D.A., Kurkov A.S., Razdobreev I.M., Fotiadi A.A.: Self-Q-switched ytterbium-doped cladding-pumped fibre laser. *Quant. Electron.* 2002 : 32, 1017-1019.
- [7] Fotiadi A.A.: Random lasers: An incoherent fibre laser. *Natur. Photon.* 2010; 4: 204-205.
- [8] Spirin V.V., Kellerman J., Swart P.L., and Fotiadi A.A.: Intensity noise in SBS with injection locking generation of Stokes seed signal. *Opt. Express.* 2006; 14: 8328-8335.
- [9] Fotiadi A.A., Kiyani R., Deparis O., Megret P., and Blondel M.: Statistical properties of stimulated Brillouin scattering in single-mode optical fibers above threshold. *Opt. Lett.* 2002; 27: 83-85.
- [10] Stokes L.F., Chodorow M., and Shaw H.J.: All-single-mode fiber resonator. *Opt. Lett.* 1982; 7:, 288-290.
- [11] Norcia S., Tonda-Goldstein S., Dolfi D., Huignard J.P., and Frey R.: Efficient single mode Brillouin fiber laser for low-noise optical carrier reduction of microwave signals. *Opt. Lett.* 2003; 28: 1888-1890.
- [12] Geng J., Staines S., Wang Z., Zong J., Blake M., and Jiang S.: Highly stable low-noise Brillouin fiber laser with ultranarrow spectral linewidth. *IEEE Photon. Technol. Lett.* 2006; 18: 1813-1815.
- [13] Molin S., Baili G., Alouini M., Dolfi D., and Huignard J.-P.: Experimental investigation of relative intensity noise in Brillouin fiber ring lasers for microwave photonics applications. *Opt. Lett.* 2008; 33: 1681-1683.
- [14] Othsubo, J.: *Semiconductor Laser. Stability, Instability and Chaos*. 2nd ed., Springer-Verlag ;Berlin; Heidelberg, 2008, 1-417.

- [15] Li X.H., Liu X.M., Gong Y.K., Sun H.B., Wang L.R., and Lu K.Q.: A novel erbium/ytterbium co-doped distributed feedback fiber laser with single-polarization and uni-directional output. *Laser Phys. Lett.* 2010; 7: 55-58.
- [16] Kim Y.-J., Chun B.J., Kim Y., Hyun S., and Kim S.-W.: Generation of optical frequencies out of the frequency comb of a femtosecond laser for DWDM telecommunication. *Laser Phys. Lett.* 2010; 7: 522-527.
- [17] Cardoza-Avendaño L., Spirin, V. V., López-Gutiérrez R.M., López-Mercado C.A., and Cruz Hernández C.: Experimental characterization of DFB and FP chaotic lasers with strong incoherent optical feedback. *Opt. Laser Technol.* 2011; 43: 949-955.
- [18] Available from: <http://www.corning.com/opticalfiber/index.as>
- [19] Thevenaz L.: Brillouin distributed time-domain sensing in optical fibers: state of the art and perspectives. *Front. Optoelectron. China.* 2010; 3: 13-21.
- [20] Spirin V.V., Lopez-Mercado C.A., Kablukov S.I., Zlobina E.A., Zolotovskiy I.O., Megret P., and Fotiadi A.A.: Single cut technique for adjustment of doubly resonant Brillouin laser cavities. *Opt. Lett.* 2013; 38: 2528-2530.
- [21] López-Mercado C.A., Spirin V.V., Kablukov S.I., Zlobina E.A., Zolotovskiy I.O., Mégret P., and Fotiadi A.A.: Accuracy of single-cut adjustment technique for double resonant Brillouin fiber lasers. *Opt. Fiber Technol.* 2014; 20: 194-198.
- [22] Spirin V.V., Lopez-Mercado C.A., Megret P., and Fotiadi A.A.: Single-mode Brillouin fiber laser passively stabilized at resonance frequency with self-injection locked pump laser. *Laser Phys. Lett.* 2012; 9: 377-380.
- [23] Debut A., Randoux S., and Zemmouri J.: Linewidth narrowing in Brillouin Lasers: Theoretical analysis. *Phys. Rev. A.* 2000; 62: 023803/1- 023803/4.
- [24] Baney D. M., and Sorin W.V.: High resolution optical frequency analysis. In: Derickson, D. (ed.) *Fiber Optic Test and Measurement*. Prentice-Hall PTR, 1998, 169-219.
- [25] Stepanov S.I., Fotiadi A.A., and Mégret P.: Effective recording of dynamic phase gratings in Yb-doped fibers with saturable absorption at 1064nm. *Opt. Express.* 2007; 15: 8832-8837.
- [26] Fotiadi A.A., Antipov O.L., and Mégret P.: Resonantly induced refractive index changes in Yb-doped fibers: the origin, properties, and application for all-fiber coherent beam combining. In: B. Pal (ed.) *Frontiers in Guided Wave Optics and Optoelectronics*. InTech, 2010; 209-234.
- [27] Lobach I.A., Kablukov S.I., Podivilov E.V., Fotiadi A.A., and Babin S.A.: Fourier synthesis with single-mode pulses from a multimode laser. *Opt. Lett.* 2015; 40: 3671-3674.
- [28] Fotiadi A.A., Antipov O.L., and Mégret P.: Dynamics of pump-induced refractive index changes in single-mode Yb-doped optical fibers. *Opt. Express.* 2008; 16: 12658-12663.

- [29] Fotiadi A.A., Zakharov N.G., Antipov O.L., and Mégret P.: All-fiber coherent combining of Er-doped amplifiers through refractive index control in Yb-doped fibers. *Opt. Lett.* 2009; 34: 3574-3576.
- [30] Fotiadi A.A., Antipov O.L., Kuznetsov M.S., Panajotov K., and Mégret P.: Rate equation for the nonlinear phase shift in Yb-doped optical fibers under resonant diode-laser pumping. *J. Holography Speckle.* 2009; 5: 299–302.
- [31] Fotiadi A., Antipov O., Kuznetsov M., and Mégret P.: Refractive index changes in rare earth-doped optical fibers and their applications in all-fiber coherent beam combining. In: A. Brignon (ed.) *Coherent Laser Beam Combining*. John Wiley & Sons, 2013, chap. 7, pp. 193-230.
- [32] Kuznetsov M.S., Antipov O.L., Fotiadi A.A., and Mégret P.: Electronic and thermal refractive index changes in Ytterbium-doped fiber amplifiers. *Opt. Express.* 2013. 21: 22374-22388.
- [33] Saleh A.A.M., and Stone J.: Two-stage Fabry-Perot filters as demultiplexers in optical FDMA LANs. *J. Lightwave Technol.* 1989; 7: 323-335.
- [34] Stadt H., and Muller J.M.: Multimirror Fabry-Perot interferometers. *JOSA A.* 1985; 2: 1363-1370.
- [35] Stepanov S.: Dynamic population gratings in rare-earth doped optical fibres. *J. Phys. D: Appl. Phys.* 2008; 41: 224002/1-224002/23.
- [36] Spirin V.V., Lopez-Mercado C.A., Kinet D., Megret P., Zolotovskiy I.O., and Fotiadi A.: A single-longitudinal-mode Brillouin fiber laser passively stabilized at the pump resonance frequency with a dynamic population inversion grating. *Laser Phys. Lett.* 2013; 10: 015102/1-015102/4.

